# Polyacene and a new class of quasi-one-dimensional conductors

S. Kivelson
*Brookhaven National Laboratory, Upton, New York 11793*
*and Department of Physics, State University of New York at Stony Brook, Stony Brook, New York 11794*

O. L. Chapman
*Department of Chemistry and Biochemistry, University of California at Los Angeles, 405 Hilgard Avenue, Los Angeles, California 90077*
(Received 7 March 1983)

Most one-dimensional conductors are quite similar since the Fermi surface is a point and the electron energy dispersion relation near the Fermi surface is linear. It is pointed out that in polyacene the Fermi surface lies at the edge of the Brillouin zone, but that an accidental degeneracy between the valence and conduction bands makes it metallic nonetheless. The dispersion relation is therefore quadratic, and the density of states diverges at the Fermi surface. Thus, polyacene $[(C_4H_2)_n]$ and its possible derivatives represent a conceptually new class of quasi-one-dimensional conductors. Moreover, we find that this class of materials has the possibility of possessing interesting condensed phases including high-temperature superconductivity and ferromagnetism.

## I. INTRODUCTION: WHAT IS POLYACENE?

In this paper we consider the properties of a novel organic polymer, polyacene $[(C_4H_2)_n]$ [Fig. 1(a)]. Polyacene is an infinite linear acene. The linear acenes from naphthalene [Fig. 1(b)] to heptacene [Fig. 1(c)] have been made.[1] Higher members of this series have proved too reactive to isolate under ordinary conditions. We believe, however, that it will be possible to work with these materials under suitable conditions.[2]

The finite length of an acene chain affects its properties in two ways. First, in the finite acenes, the energy levels are discrete. Most importantly, this results in a gap between the highest-lying occupied $\pi$ orbital and the lowest-lying unoccupied $\pi$ orbital. This gap decreases as one goes up the series from naphthalene to heptacene.[1] Let us obtain a crude theoretical estimate of the typical spacing $\Delta E$ between levels near the Fermi surface for a chain of $N$ monomers. As we shall see, the energy is a quadratic function of the wave vector $k$ and so $\Delta E \sim W/N^2$, where $W \approx 10$ eV is the $\pi$-band width. For $N$ sufficiently large that $\Delta E$ is small compared to other characteristic energies (most importantly compared to the transition temperature $kT_c$ to the low-temperature ordered phase) the spectrum can be treated as a continuum. The second finite-length effect is that the chemical nature of the chain ends affects the bond-alternation pattern of the molecule. In principle, this effect could be eliminated if a cyclic polymer [Fig. 1(d)] could be synthesized.[2]

In this paper we will discuss the qualitative features of the electronic properties of the infinite polyacene. Since it has not yet been synthesized our discussion is necessarily speculative and hence we confine ourselves, as much as possible, to conclusions that follow directly from the symmetries of the molecule. However, to make our discussion more concrete we will consider a microscopic model of polyacene in the same spirit as the model of polyacetylene $[(CH)_n]$ considered by Su, Schreiffer, and Heeger.[3] Indeed, the fact that polyacene and polyacetylene have all the same constituents and that polyacene can be viewed as

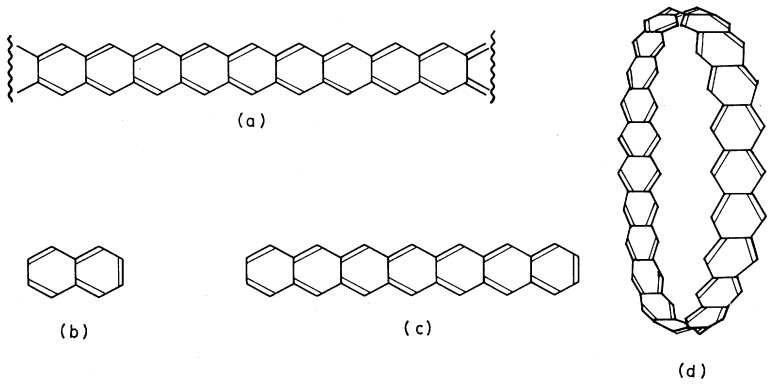


FIG. 1. (a) Polyacene $[(C_4H_2)_n]$; (b) naphthalene $[(H_2(C_4H_2)C_6H_4)]$; (c) heptacene $[(H_2(C_4H_2)_6C_6H_4)]$; (d) a cyclic polyacene.

 

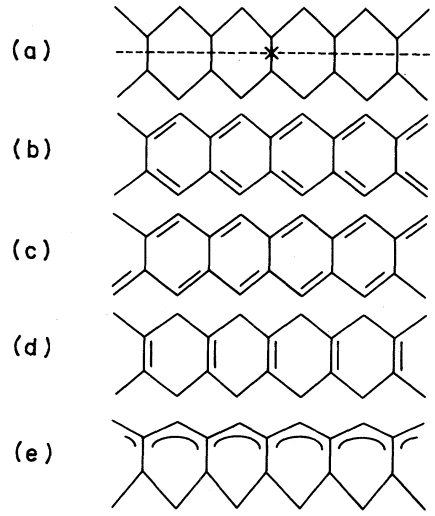


FIG. 2. Schematic structures of polyacene: (a) the undistorted molecule; (b)—(d) possible symmetric Peierl's distortions; (e) antisymmetric Peierl's distortion. Double lines represent relatively short bonds.

two parallel chains of polyacetylene bound together implies that the microscopic physics in the two materials is quite similar. Moreover, in both materials the $\pi$ band, in which the interesting physics occurs, is half full. However, the different symmetries of the two molecules result in dramatically different low-temperature condensed states. In fact, the Fermi-surface electronic structure of polyacene is quite different from that of any quasi-one-dimensional conductor studied to date. It is this observation that makes it an especially interesting material to study. We show that the chemically most natural sort of Peierl's instability [shown in Figs. 2(b) and 2(c)] is suppressed, which leaves open the possibility that polyacene could exhibit some other high-temperature condensed phase. In particular we show that there is a possibility that polyacene could be a superconductor.

The search for an organic superconductor has been largely frustrated by the fact that, in one dimension, the superconducting transition is usually preempted by a Peierl's transition which produces a lattice distortion with period $2k_F$. The new lattice periodicity causes the Fermi surface to fall at the edge of the new Brillouin zone and hence opens a gap at the Fermi surface. The existence of a Peierl's instability is a consequence of the perfect nesting of the Fermi surface in one dimension. If we imagine that we impose a pattern of lattice distortion with period $2k_F$ and magnitude $u_0$, then the resulting potential produces scattering between the nearly degenerate particle and hole states on opposite sides of the Fermi surface. As a result, the total electronic energy per atom $E_{\rm el}(u_0)$ is a nonanalytic function of $u_0$ which varies faster than $u_0^2$ for small $u_0$. It is easy to show[3] that $E_{\rm el}(u_0)=E_0 - Au_0^2\ln(a^2/u_0^2)+\cdots$, where $a$ is a lattice constant and $A=\alpha^2/Zt_0$ with $\alpha$ as a characteristic electron-phonon coupling constant and $Zt_0$ the electron bandwidth. The electronic energy gained for finite $u_0$ thus always exceeds the cost in lattice strain energy, $E_{\rm strain}=\frac{1}{2}K(u_0)^2+\cdots$.

Although organic superconductors[4] such as $(TMTSF)_2X$ (ditetramethyltetraselenafulvalenium salts) have been found, they may be considerably more three dimensional than other organic conductors. The three-dimensional band structure tends to spoil the Fermi-surface nesting and hence suppresses the Peierl's instability.[5]

## II. THE ELECTRONIC STRUCTURE OF POLYACENE

Polyacene, being a single polymeric chain, is expected to be highly anisotropic. However, because of its unit-cell structure, the Fermi surface already lies at the edge of the Brillouin zone, even in the undistorted molecule shown in Fig. 2(a). Normally, this would mean that polyacene would be an insulator. However, an accidental near-degeneracy at the Fermi surface results in metallic behavior nonetheless. To see this, we calculate the band structure of the material in a simple tight-binding approximation in which we consider explicitly only one electronic orbital per site corresponding to the out-of-plane carbon $P$ orbital. The energy eigenstates can be labeled by a Bloch wave number $-\pi/2a<k<\pi/2a$ and a parity index $\lambda=\pm1$ which indicates whether the state is symmetric ($\lambda=1$) or antisymmetric ($\lambda=-1$) under reflection through the plane bisecting the molecule lengthwise [the dashed line in Fig. 2(a)]. Alternatively, for some purposes it is more convenient to label the states $\lambda_R=\pm1$ depending on their transformation properties under reflection about a point [indicated by a cross in Fig. 2(a)] halfway up one of the vertical bonds. In the undistorted molecule the two descriptions are equivalent. Although there are four atoms per unit cell, the reflection symmetry reduces the Hamiltonian at fixed $k$ to a $2\times2$ matrix. The general solution can be written in the form

$$E_\lambda(\pm1,k)=-\frac{\bar{\epsilon}_\lambda(k)}{2}\pm\left[\left[\frac{\epsilon_\lambda(k)}{2}\right]^2+[t_g(k)]^2\right]^{1/2}, \quad (1)$$

where the $+$ $(-)$ refers to the conduction (valence) band and $\bar{\epsilon}$, $\epsilon$, and $t$ are the Fourier transforms of the various combinations of tight-binding matrix elements (given ex-

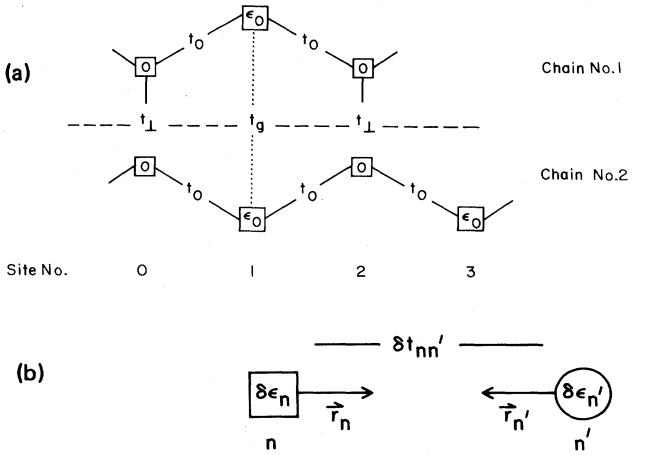


FIG. 3. Schematic representation (a) of the tight-binding electronic Hamiltonian and (b) of the electron-phonon coupling. See description in text.

plicitly in the Appendix) which, in general, are even functions of $k$ with $t_\lambda(\pi/2a)=0$.

In the simplest version of the theory we retain only couplings out to nearest neighbors, as shown in Fig. 3(a). (We call this the nearest-neighbor model.) We define the zero of energy such that the site energy on all odd-numbered sites is zero. The site energy on even-numbered sites is $-\epsilon_0$ which may be slightly different from zero. The off-diagonal matrix element between neighboring sites on a single chain is $t_0 \approx 2.5$ eV which we expect to be of roughly the same magnitude as the matrix element between even sites on the two different chains, $t_\perp$. For this model, $\bar{\epsilon}_\lambda(k)=(\epsilon_0+\lambda t_\perp)$, $\epsilon_\lambda(k)=\epsilon_0+\lambda t_\perp$, and $t_\lambda(k)=2t_0\cos(k)$. The band structure for this model is shown in Fig. 4(a). As can be clearly seen, there is a degeneracy between the highest-lying occupied (negative energy) state and the lowest-lying empty (positive energy) state.

This degeneracy is possible because the two bands which are degenerate at the Fermi surface have different parity. Since this degeneracy is essential to obtain conducting behavior, it is worth examining the nature of the zero-energy Fermi-surface states. They are shown schematically in Figs. 4(b) and 4(c). They are the even- and odd-parity standing-wave states with $k=\pi/2a$ and zero amplitude on all even-numbered sites. The degeneracy of these two states is accidental. However, it is only when one includes much-farther-neighbor (hence much smaller) tight-binding matrix elements in the model that the degeneracy at $k=\pi/2a$ is destroyed. The first such matrix element is the fourth-neighbor interaction, $t_g$, shown as a dashed line in Fig. 3(a). This term splits the even- and odd-parity states by an amount $2t_g$. If $t_g$ has the same sign as $t_\perp$ (which seems likely), then the effect of including $t_g$ is to cause the even and odd bands to cross [see Fig. 5(a)]. If $t_g$ has the opposite sign to $t_\perp$, then $t_g$ opens a gap at the Fermi surface. In which follows, we will assume that $t_g$ is small and has the same sign as $t_\perp$. Thus, we can treat the nearest-neighbor model as a first-order approximation and then correct our results to include the effects of farther-neighbor interactions.

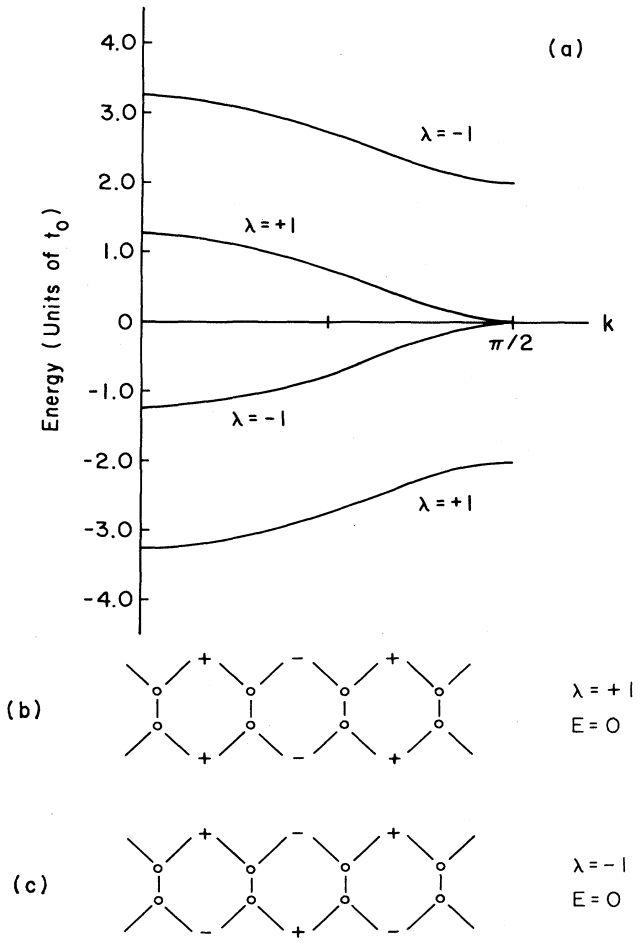


FIG. 4. Electronic states in polyacene. (a) Band structure of the undistorted molecule. (b) and (c), wave functions of the Fermi-surface states.

The result of having the Fermi surface lie at the edge of the Brillouin zone is anomalous behavior of the electron gas. Typically, the energy dispersion relation near the Fermi surface is of the form $E_k=\hbar V_F(|k|-k_F)$, but in polyacene,

$$E_{k,\Lambda}=\Lambda\frac{\hbar^2}{2m_\Lambda}(k-k_F)^2\,, \tag{2}$$

where $\Lambda=+1$ for the conduction band and $-1$ for the valence band and $m_\Lambda=\hbar^2(t_\perp-\Lambda\epsilon_0)/(4t_0)^2$. As a result, the density of states diverges in the vicinity of the Fermi surface:

$$\rho_\Lambda(E)=\frac{4\sqrt{2m_\Lambda}}{\hbar}\frac{1}{\sqrt{|E|}}. \tag{3}$$

Although three-dimensional effects (interchain coupling) and farther-neighbor interactions such as $t_g$ will tend to round out this divergence, we expect polyacene to have a very large density of states at the Fermi surface and hence unusually strong instabilities.

To explore these instabilities, we must include electron-phonon and direct electron-electron interactions in our

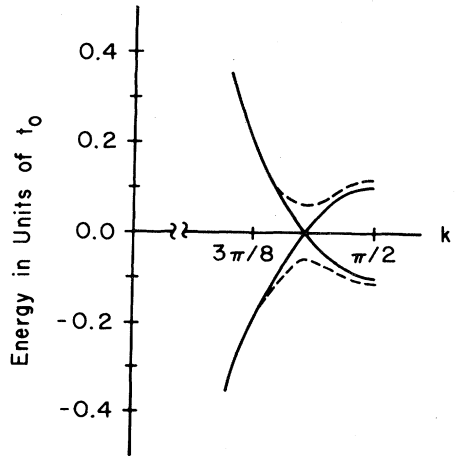


FIG. 5. Band structure near the edge of the Brillouin zone including the effect of farther-neighbor interactions: (—), in the undistorted molecule; (———), for a distorted molecule of the sort shown in Fig. 2(e).

model of polyacene. Consistent with our approach so far, we include electron-phonon interactions in a tight-binding approximation keeping only interactions between nearest-neighbor sites. There are two sorts of electron-phonon interactions consistent with the symmetry of the molecule which we call generically $\alpha$ and $\beta$. Imagine that the two sites $n$ and $n'$ are originally separated by $\vec{R}$ and that we displace them a distance $\vec{r}_n$ and $\vec{r}_{n'}$, respectively, as shown in Fig. 3(b). The hopping matrix $t$ between sites $n$ and $n'$ is thereby increased by an amount $\delta t_{n,n'}=\alpha\vec{R}\cdot(\vec{r}_n-\vec{r}_{n'})$ and the site energy of an electron on site $n$ is increased by an amount $\delta t_n=\beta\hat{R}\cdot(\vec{r}_n-\vec{r}_{n'})$ where $\hat{R}=\vec{R}/R$.

By analogy with the Su, Schrieffer, and Heeger[3] (SSH) model of polyacetylene we expect $\alpha\approx 4$—$6$ eV/Å. It is harder, but, as we shall see, more important to obtain a realistic estimate of $\beta$. If we consider the change in the energy of a free-electron gas with respect to a change in volume at densities corresponding to a carbon atom, we find that $\beta\approx 3$ eV/Å. Other methods lead to rather higher values of $\beta$.

It is a somewhat more perplexing problem to treat the electron-electron interactions correctly. In the same tight-binding spirit that has motivated our model to this point, the interactions could be treated within the context of an extended Hubbard model. However, the correct magnitude of the interaction strengths that enter such a model is still controversial. It is argued in Ref. 6 that the interactions are probably weak in $(CH)_x$ and can be ignored as a zeroth-order approximation if we renormalize the effective parameters that enter the noninteraction Hamiltonian. Thus, for the purpose of this paper, we will only make very general observations concerning the possible effects of weak electron-electron interactions, and hence will never need to consider an explicit model.

## III. CONDENSED STATES

### A. The Peierl's instability

Let us first examine the Peierl's instabilities with period $2k_F$. The possible patterns of lattice distortion are shown schematically in Figs. 2(b)—2(e). The double lines here are taken to represent bonds that are slightly shorter than in the undistorted molecule, and the single lines represent bonds that are slightly longer. To determine which of these distortions is energetically favorable at zero temperature, we must calculate the total adiabatic potential energy as a function of the magnitude of the dimensionless lattice order parameter $\Delta$. ($\Delta$ is, in each case, proportional to the magnitude of the lattice disortion times the appropriate electron-phonon coupling constant.) The patterns of lattice distortion in Figs. 2(b)—2(d) are all even under reflection, and so cause no mixing between the nearly degenerate states at the Fermi surface. As a result, the electronic energy $E_{\rm el}(\Delta)$ is an analytic function of $\Delta$ near $\Delta=0$, in contrast with the normal Peierl's case. For the pattern of lattice distortion shown in Figs. 2(b) and 2(c), $E_{\rm el}$ is an even function of $\Delta$, $E_{\rm el}\sim -1/2k^{\rm eff}\Delta^2+O(\Delta^4)$ and hence the distortion is disfavored unless the electron-phonon coupling constant is sufficiently strong that $k_{\rm eff}$ is greater than the lattice stiffness constant $k$. For the nearest-neighbor-only model, $(k_{\rm eff}/k)\approx 1$ for reasonable values of the various coupling constants (see the Appendix). Including farther-neighbor terms, such as $t_g$, results in a small reduction of this ratio. Moreover, since quantum fluctuations of the lattice[7] tend to oppose the lattice distortion, we conclude that this type of bond alternation probably does not occur in polyacene. Note that this conclusion is strongly contrary to usual chemical intuition. Note further that this explains the remarkable difference between the behavior of long polyacenes and chemically similar polyacetylene. Bond alternation analogous to that shown in Figs. 2(b) and 2(c) is responsible[3] for the band gap, $\Delta\approx 1.5$ eV, observed in long polyacetylenes. It is the absence of such bond alternation that explains the small size of the gap in polyacenes with even as few as seven monomer units.

In Fig. 1(d), $E_{\rm el}\sim A\Delta$, and hence there is a tendency for the molecule to become more narrow. However, this sort of distortion does not open a gap in the electronic spectrum; it merely changes the values of $t_\perp$ and $\epsilon_0$ a little. We will imagine that this distortion has already been taken into account in defining $t_\perp$ and $\epsilon_0$.

Only the distortion in Fig. 1(e) breaks the reflection symmetry of the molecule. Again, $E_{\rm el}(\Delta)$ must be an even function of $\Delta$, but because of the mixing between the nearly degenerate states in the valence and conduction bands it need not be analytic. Indeed, because of the $1/\sqrt{|E|}$ divergence in the density of states at the Fermi surface, $E_{\rm el}(\Delta)$ is a more rapidly increasing function of $\Delta$ for small $\Delta$:

$$E_{\rm el}(\Delta)=-k^{\rm eff}|\Delta|^{3/2}[1+O(|\Delta|)]\ . \tag{4}$$

$k^{\rm eff}$ can be calculated explicitly for the nearest-neighbor model (see Appendix): $k_{\rm eff}\approx\frac{8}{3}\sqrt{2t_0t_\perp}$ where $\Delta=2\beta u_0/t_0$ and $u_0$ is the distance that the odd-numbered atoms move. Since, for small $|\Delta|$, the amount of electronic energy gained always exceeds the strain energy ($\sim\Delta^2$), there is an absolute instability at zero temperature. If we include farther-neighbor interactions, the dependence of $E_{\rm el}$ on $\Delta$ becomes less strong. There is, however, still a logarithmic singularity of the usual Peierl's sort, and it is particularly strong because of the large (but no longer infinite) density of states. It is shown in the Appendix that for $t_g>2t_0|\Delta|$, $E_{\rm el}(\Delta)\sim k_{\rm eff}(\sqrt{t_0/t_g})\Delta^2\ln|\Delta|$.

Although formally no phase transition can occur in the one-dimensional model we have considered until now, we know that interchain interactions will tend to stabilize the Peierl's state at finite temperatures.[8] To obtain a crude estimate of this temperature, we calculate implicitly the mean-field transition temperature $T_p$ according to the usual BCS formula[5]

$$1=-2g\int d\epsilon[\rho(\epsilon)/8\epsilon]\tanh(\epsilon/2kT_p)\ , \tag{5}$$

where $g=(h\beta^2/\omega_0 M)D(0)=-2\beta^2/M\omega_0^2$, in which $D(\omega)$ is the phonon propagator, $M$ is the ion mass, and $\omega_0$ is the optical phonon frequency. In the nearest-neighbor model with weak coupling ($g/2t_0\ll 1$) Eq. (5) yields

$$kT_p\approx t_0(g/t_0)^2\ . \tag{6}$$

Because of the divergence of the density of states, $kT_p$ depends much less strongly on $g$ than the usual exponential dependence $[T_p \sim \exp(-t_0/g)]$. This implies that the transition temperature can be quite high. (We estimate $g \gtrsim \frac{1}{2}$ eV so $kT_p \sim 0.1$ eV.) If $t_g > kT_p$, then including farther-neighbor interactions will reduce the transition temperature substantially.

Note that it is only the on-site interaction $\beta$ which enters Eqs. (4) and (5). This is because the states at the Fermi surface have vanishing amplitude on all even-numbered sites so the off-diagonal coupling proportional to $\alpha$ vanishes at the Fermi surface.

### B. Other instabilities

The same electron-phonon interactions can produce a superconducting instability. The coupling constants that determine the mean-field superconducting transition temperature are the same as those that determine the Peierl's instability. Naively one might suppose that this implies that the Peierl's instability supercedes the superconductivity instability since the cutoff energy [the high-energy cutoff in Eq. (5)] which enters the expression for the Peierl's transition temperature is the Fermi energy while it is the optical-phonon frequency $\hbar\omega_0$ for the superconducting transition. This conclusion is not justified for several reasons. First, if we consider the Eliashberg equation[9] for the superconducting transition temperature, we find that for polyacene the coupling is strong, and hence the cutoff dependence of the theory is not of the simple BCS form. Indeed, electrons with energies large compared to $\hbar\omega_0$ contribute substantially to the superconducting transition. Second, because the interaction strengths are equal, the superconducting and Peierl's order parameters must be treated on an equal footing, even at the level of mean-field theory. Finally, since in a proper treatment of the model the interchain coupling is essential to the existence of long-range order, it may be important to treat the effects of the true one-dimensional fluctuations and the interchain interactions in a more careful way. Work in this direction is in progress.[10] At the current level of theory, all we can conclude is that the Peierl's and superconducting transition temperatures are equal to each other within the large theoretical uncertainty.

Finally, we note that there is the possibility of a magnetically ordered ground state if the electron-electron repulsions are the dominant interactions. If, for simplicity, we treat only an on-site electron-electron repulsion $U$ (Hubbard $U$), then for small $U$, the mean-field or unrestricted Hartree-Fock ground state can be either ferromagnetic or antiferromagnetic. The former possibility is unusual and occurs here due to the divergent density of states.

## IV. CONCLUSIONS

In conclusion we have shown that polyacene is expected to be an unusual one-dimensional conductor with a novel electronic structure. Because of this structure, polyacene and, we hope, other molecules with similar symmetries may be expected to behave rather differently than the other quasi-one-dimensional conductors that have been studied to date. In particular, the presence of a divergent density of states (or, in a more realistic model, a very large density of states) at the Fermi energy implies that polyacene will have a broken-symmetry condensed phase with a rather high transition temperature (probably in excess of room temperature). By analogy with $(CH)_x$ we feel that this phase most likely involves the electron-phonon interaction, and is hence either a superconducting or an antisymmetric ferroelectric Peierl's phase.

*Note added.* An earlier quantum-chemical calculation (Ref. 11) of the properties of polyacene which uses a somewhat larger basis than the present calculation produces a band structure remarkably similar to that in Figs. 3 and 5. In Ref. 11 it was concluded that a distortion of type b or c is slightly energetically favorable. This is consistent with our results. However, as discussed previously, we expect this instability to be superceded by one of the other analytically stronger instabilities such as the antisymmetric Peierl's instability. See also Ref. 12.

## ACKNOWLEDGMENTS

One of us (S.K.) would like to acknowledge the hospitality of Brookhaven National Laboratories and the support of the U.S. Department of Energy, Contract No. DE-AC02-76CH00016. We would also like to acknowledge National Science Foundation Grant No. CHE81-1196.

## APPENDIX: DETAILS

### 1. The undistorted molecule

In this section we consider the band structure of the undistorted infinite polyacene. We start with a noninteracting tight-binding Hamiltonian with one orbital per site (carbon) with the symmetry of the out-of-plane $p$ orbital. The model is the most general one consistent with the symmetries of the molecule:

$$H = -\sum_s \sum_{a=1}^{2} \sum_n \sum_{m\geq 0} I(n \mid m)(C^\dagger_{a,n,s} C_{a,n+m,s} + \text{H.c.}) - \sum_s \sum_n \sum_m J(n \mid m)(C^\dagger_{1,n,s} C_{2,n+m,s} + \text{H.c.}) , \quad \text{(A1)}$$

where $C^\dagger_{a,n,s}$ creates an electron of spin $s$ on the $n$th carbon on chain $a$. $I$ and $J$ are, respectively, the inter- and intrachain matrix elements. We are free to choose the phases of the orbitals such that $J$ and $I$ are real and hence $I(n \mid m) = I(n+m \mid -m)$ and $J(n \mid m) = J(n+m \mid -m)$. Since the molecule is translationally invariant, $I$ and $J$ depend only on whether $n$ is even or odd: $I(n \mid m) = I(n+2j \mid m)$ and $J(n \mid m) = J(n+2j \mid m)$.

The eigenstates of the Hamiltonian can be taken to be the Bloch waves

$$|k,\lambda,\Lambda,s\rangle = \sum_{a=1}^{2} (\lambda)^a {\sum_n}' \frac{e^{2ikn}}{\sqrt{2N}} [\alpha_\Lambda(\lambda,k) C^\dagger_{a,2n,s} + \beta_\Lambda(\lambda,k) e^{ik} C^\dagger_{a,2n+1,s}] |0\rangle , \quad \text{(A2)}$$

where $|0\rangle$ is the vacuum, $\lambda=+1$ $(-1)$ if the state is even (odd) under reflection, $\Lambda=+1$ $(-1)$ for the conduction (valence) band, and we have chosen units of length $a=1$. The energy eigenvalues are obtained by solving the $2\times2$ matrix equation

$$\{E+\tfrac{1}{2}\bar{\epsilon}_\lambda(k)+\tfrac{1}{2}\epsilon_\lambda(k)\sigma_z+t_\lambda(k)\sigma_x\}\begin{bmatrix}\alpha\\ \beta\end{bmatrix}=0\ ,$$

where $\sigma_a$ are the Pauli matrices,

$$t_\lambda(k)=\sum_m{}'e^{(2m+1)ik}[I(0\,|\,2m+1)+J(0\,|\,2m+1)]\ ,$$

$$\bar{\epsilon}_\lambda(k)=\sum_m{}'e^{2mik}[I(0\,|\,2m)+\lambda J(0\,|\,2m)+I(1\,|\,2m)+\lambda J(1\,|\,2m)]\ , \tag{A3}$$

and

$$\epsilon_\lambda(k)=\sum_m{}'e^{2mik}[I(0\,|\,2m)+\lambda J(0\,|\,2m)-I(1\,|\,2m)-\lambda J(1\,|\,2m)]\ .$$

The energy eigenvalues $E_\lambda(\Lambda,k)$ of this equation are given in Eq. (1).

Since $I$ and $J$ are real, $t$, $\epsilon$, and $\bar{\epsilon}$ are real even functions of $k$. To study the behavior of the energy near the edge of the Brillouin zone, we consider the dependence of the energy on $q=\pi/2-|k|$ $(q\geq0)$. Since $I$ and $J$ are even functions of $m$, $t$ is easily seen to be an odd function of $q$, which vanishes at the zone edge $(q=0)$, and $\epsilon$ and $\bar{\epsilon}$ are even functions of $q$. We note further that since we are free to choose an arbitrary zero of energy we can do it in such a way that $E_1(1,\pi/2)=-E_{-1}(-1,\pi/2)$. Since, in general, we expect the nearest-neighbor hopping matrix elements $I(0\,|\,1)=t_0$ and $J(0\,|\,0)=t_\perp$ to be the largest matrix elements (we assume $t_\perp>0$), our choice of the zero of energy is such as to ensure that

$$\sum_m(-1)^mI(1\,|\,2m)=0\ .$$

With this definition, it is easy to see that near the Fermi surface

$$E_\lambda(\lambda,k)=\lambda\left[-\bar{\epsilon}+\frac{(\hbar q)^2}{2m_\lambda}+O(q^4)\right]\ , \tag{A4}$$

where

$$\bar{\epsilon}=-\tfrac{1}{2}[\bar{\epsilon}_{-1}(\pi/2)+|\epsilon_{-1}(\pi/2)|]=\sum_m(-1)^mJ(1\,|\,2m) \tag{A5}$$

and

$$\frac{h^2}{2m_\lambda}=\frac{(A_\lambda)^2}{|\epsilon_\lambda(\pi/2)|}-\tfrac{1}{2}B_\lambda\approx\frac{(2t_0)^2}{(t_\perp-\lambda\epsilon_0)}\ , \tag{A6}$$

where

$$A_\lambda=-\sum_m(2m+1)(-1)^m\times[I(0\,|\,2m+1)+\lambda J(0\,|\,2m+1)] \tag{A7}$$

and

$$B_\lambda=-\sum_m(2m)^2(-1)^m[J(1\,|\,2m)+\lambda I(1\,|\,2m)]\ . \tag{A8}$$

If $\bar{\epsilon}$ is greater than zero the two bands cross, while for $\bar{\epsilon}<0$ a gap of $2\bar{\epsilon}$ appears between the valence and conduction bands. As stated in the text, the most important contribution to $\bar{\epsilon}$ is $\bar{\epsilon}\approx J(1\,|\,0)=t_g$.

### 2. Electron-phonon coupling

There are three lattice degrees of freedom per carbon atom and three per hydrogen atom. Of these, the motion of the hydrogen is only weakly coupled to the $\pi$-electronic structure and the motion of the carbon atom out of the plane of the molecule couples only in second order in the magnitude of the lattice displacement. Thus, we can concentrate our attention to the two in-plane degrees of freedom $u_{a,n}$ and $v_{a,n}$, where $u_{a,n}$ is the displacement of the $n$th atom on chain $a$ in the in-chain direction and $v_{a,n}$ is the displacement of the same atom perpendicular to the chain direction. In terms of these coordinates, the patterns of lattice distortion shown in Figs. 2(b)—2(e) correspond to the following displacements:

$$\begin{aligned}&\text{(b)}\ u_{a,n}=(-1)^nu_0,\ v_{a,n}=0\ ,\\ &\text{(c)}\ u_{a,n}=(-1)^a(-1)^nu_0,\ v_{a,n}=0\ ,\\ &\text{(d)}\ u_{a,n}=0,\ v_{a,n}=(-1)^a\bar{v}\ ,\\ &\text{(e)}\ u_{a,n}=0\ ,\ v_{a,n}=(-1)^nv_0\ .\end{aligned} \tag{A9}$$

A lattice distortion results in a change in the electronic structure through changes in the $I$'s and $J$'s of the preceding section. Thus, the electron-phonon coupling is of the form

$$H_{e\text{-ph}}=-\sum_s\sum_a\sum_n\sum_{m\geq0}\delta I_a(n\,|\,m;\{u\},\{v\})(c^\dagger_{a,n,s}c_{a,n+m,s}+\text{H.c})-\sum_s\sum_n\sum_m\delta J(n\,|\,m;\{u\},\{v\})(c^\dagger_{l,n,s}c_{2,n+m,s}+\text{H.c.})\ , \tag{A10a}$$

where $\delta I$ and $\delta J=0$ in the absence of lattice distortion. It is possible to find the electronic states of the distorted lattice in the same generality as in the preceding section. For lattice distortions of types (b) and (d), the energy eigenstates are form as in the undistorted molecule [Eq. (A2)] and the energies can be determined by diagonalizing a $2\times2$ matrix. The energy eigenstates for the pattern of lattice distortion (c) are of the form

$$|k,\lambda,\Lambda,s\rangle=\sum_n{}'\frac{e^{2ikn}}{\sqrt{2N}}[\alpha_\Lambda(\lambda,k)c^\dagger_{1,2n,s}+\beta_\Lambda(\lambda,k)e^{ik}c^\dagger_{1,2n+1,s}+\lambda\alpha^*_\Lambda(\lambda,k)c^\dagger_{2,2n,s}+\lambda\beta^*_\Lambda(\lambda,k)e^{ik}c^\dagger_{2,2n+1,s}]|0\rangle \quad \text{(A10b)}$$

and the energies can be found without great difficulty. Since the pattern of lattice distortion (e) breaks the reflection symmetry of the molecule, the energy eigenvalues must be obtained by solving a $4\times4$ matrix equation. This could be done, at least numerically. In all cases, the difference in energy between the distorted and undistorted lattice configurations, $\Delta E$, can be obtained by integrating over the full bands. ($\Delta E$ is defined to be the change in energy per monomer.) The resulting expressions are generally quite complicated. However, we are primarily interested in the leading-order behavior of $\Delta E$ when the magnitude of the lattice displacement is small. This dependence can be obtained either by expanding the exact expression for the energy in powers of the lattice displacement or, more simply, by calculating the energy using perturbation theory [Brillouin-Wigner perturbation theory in case (e)].

We have calculated $\Delta E$ in both ways. In order to calculate $\Delta E$ exactly, we have considered the nearest-neighbor model with tight-binding electron-phonon couplings of the sort described in the text (e.g., for patterns (b) and (c) $\delta I_a(n\,|\,m)=\delta_{m,1}(-\lambda)^n 1\alpha u_0$ and $\delta J(n\,|\,m)=0$ where $\lambda=+1$ for (b) and $-1$ for (c), while for pattern (e) $\delta I_a(n\,|\,m)=(-1)^a[\delta_{m,0}(-1)^n 4\beta v_0+\delta_{m,1}(-1)^n 2\alpha v_0/\sqrt{3}]$ and $\delta J(n\,|\,m)=0$). The perturbative results are simpler to understand and make it clear that the results do not depend on the details of the model. For either pattern (b) or (c), $\Delta E$ is given to second order by the expression

$$\Delta E=-\frac{2}{N}\sum_k\sum_{\lambda=\pm1}\frac{|\langle k,\lambda,1\,|\,H_{e\text{-ph}}\,|\,k,\lambda,-1\rangle|^2}{E_1(\lambda,k)-E_{-1}(\lambda,k)} \quad \text{(A11a)}$$

$$\approx-\frac{4(2\alpha)^2u_0^2}{\bar{E}}\,, \quad \text{(A11b)}$$

where in the second line we have replaced the matrix element by its value at the Fermi surface

$$\langle k_F,\lambda,1\,|\,H_{e\text{-ph}}\,|\,k_F,\lambda,-1\rangle=2\alpha u_0 \quad \text{(A12)}$$

and the energy denominator by an average value $\bar{E}$. With a little work it is possible to show that the exact result for the nearest-neighbor model is of the form (A11b) with

$$\frac{1}{\bar{E}}=\frac{x[K(x^2)-E(x^2)]}{\pi t_0}\approx\frac{1}{t_0+t_\perp}\,, \quad \text{(A11c)}$$

where $x^2=1+(t_\perp/4t_0)^2$ and $K(x^2)$ and $E(x^2)$ are, respectively, the complete elliptic integrals of the first and second kind and, for simplicity, we have taken $\epsilon_0=0$. Thus $k_{\text{eff}}$, as described in the text, is $k_{\text{eff}}/k=(2\alpha)^2/t_0K\approx1$ for SSH values of the parameters, $\alpha\approx4$ eV/Å, $t_0=2.5$ eV, and $K=20$ eV/Å$^2$.

For the pattern of lattice distortion (e) we must treat the coupling between the nearly degenerate states carefully. To obtain the leading-order contribution to $\Delta E$, we need keep only this coupling. First, let us obtain the one-electron energies $\epsilon_\Lambda(k)$ of the states in the two bands near the Fermi surface (see Fig. 5):

$$\epsilon_\Lambda(k)=\tfrac{1}{2}E_+(k)+\Lambda\{[\tfrac{1}{2}E_-(k)]^2+(\Delta_k)^2\}^{1/2}+O((\alpha v_0)^2/t_\perp)\,, \quad \text{(A13)}$$

where $\Lambda=\pm1$, $E_\pm(k)=E_1(1,k)\pm E_{-1}(-1,k)$, $\Delta_k=\langle k,1,1\,|\,H_{e\text{-ph}}\,|\,k,-1,-1\rangle$, and the term $O((\alpha v_0)^2/t_\perp)$ reflects the coupling to the two bands that are far from the Fermi surface. This term must then be summed over $k$. Since the dominant contribution to $\Delta E$ comes from $k$ near $k_F$, we can replace $E_\lambda(\lambda,k)$ by its small $q=k_F-|k|$ value [Eq. (A4)] and the matrix elements $\Delta k$ by their value for $k=k_F$:

$$\langle k_F,1,1\,|\,H_{e\text{-ph}}\,|\,k_F,-1,-1\rangle=4\beta v_0\,. \quad \text{(A14)}$$

The resulting expression for $\Delta E$ is

$$\frac{d(\Delta E)}{d\Delta}=-\frac{4t_0}{\pi}\frac{2\bar{m}t_0}{\hbar^2}[\sqrt{\Delta}f(x)]+\Delta \approx-\frac{2t_0}{\pi}[\sqrt{\Delta}f(x)]+\Delta\,, \quad \text{(A15)}$$

where $\Delta\equiv2\beta v_0/t_0$, $1/\bar{m}$ is the average effective mass $1/\bar{m}=\frac{1}{2}(1/m_1+1/m_2)$ [$\hbar^2/m_\lambda\approx8(t_0)^2/t_\perp\approx8t_0$], $x=\bar{\epsilon}/(4\beta v_0)$ with $\bar{\epsilon}\approx t_g$ as in Eq. (A5), and

$$f(x)=\int_0^\infty dy\,[(x-y^2)^2+1]^{-1/2}\,. \quad \text{(A16a)}$$

Important limits of $f$ are its value in the nearest-neighbor model

$$f(0)=\frac{4}{25\sqrt{\pi}}[\Gamma(\tfrac{5}{4})]^2 \quad \text{(A16b)}$$

and its value when $t_g\gg4\beta v_0$

$$f(x)\sim\ln(8x)/\sqrt{x}\,. \quad \text{(A16c)}$$


[1]E. Clar, *Polycyclic Hydrocarbons* (Academic, New York, 1964), Vol. I, Chap. 10; W. J. Bailey and Chien-Wei Liao, J. Am. Chem. Soc. 77, 992 (1955).

[2]O. Chapman (unpublished).

[3]W. P. Su, J. R. Schreiffer, and A. J. Heeger, Phys. Rev. Lett. 42, 1698 (1979); Phys. Rev. B 22, 2099 (1980); 28, 1138(E) (1983).

[4]For example, see S. S. P. Parkin, M. Ribault, D. Jérome, and K. Blechgaard, J. Phys. C 14, 5305 (1981).

[5]B. Horovitz, Phys. Rev. B 16, 3945 (1977); Solid State Commun. 18, 445 (1976).

[6]S. Kivelson and D. E. Heim, Phys. Rev. B 26, 4278 (1982).

[7]W. P. Su, Solid State Commun. 35, 899 (1980).

[8]P. Lee, M. Rice, and P. W. Anderson, Phys. Rev. Lett. 31, 462

(1973); H. Gutfreund, B. Horovitz, and M. Weger, Phys. Rev. B 12, 3174 (1975).
[9]G. M. Eliashberg, Zh. Eksp. Teor. Fiz. 38, 966 (1960) [Sov. Phys.—JETP 11, 696 (1960)].
[10]S. Kivelson and B. Mitrovic (unpublished).
[11]M.-H. Whango, R. Hoffman, and R. B. Woodward, Proc. R. Soc. London, Ser. A 366, 23 (1979).
[12]M. Kertesz and R. Hoffman (unpublished).